THz Multi-Layer Imaging via Nonlinear Inverse Scattering

A. Bose*†, A. Kadu*‡, H. Mansour*, P. Wang*, P. Boufounos*, P. V. Orlik*, and M. Soltanalian†
* Mitsubishi Electric Research Laboratories, Cambridge, MA 02139, USA.
† University of Illinois at Chicago, Chicago, IL 60607, USA.
‡ Utrecht University, Utrecht, The Netherlands.

***Abstract*—In this paper, we address the problem of mitigating nonlinear shadow effects in Terahertz time-domain spectroscopy (THz-TDS) multi-layer imaging. To that end, we utilize a one-dimensional (1D) nonlinear model to capture the interaction between the dielectric permittivity profile and the THz wavefield and recover the multi-layer structure by solving a 1D nonlinear inverse scattering via iterative and sequential optimization over frequencies. Numerical results confirm the effectiveness of the proposed method.**

I. Introduction and Problem of Interest

In the recent years, electromagnetic (EM) waves in Terahertz (THz) frequencies have attracted considerable amount of interest in imaging, gas sensing, non-destructive evaluation (NDE), security screening and many other applications due to their noninvasive, noncontact, and nonionizing characteristics [1]–[3].

To image a multi-layer sample, a THz time-domain spectroscopy (THz-TDS) system, shown in Fig. 1 (a), sends an ultra-short pulse (1-2 picoseconds) in a raster scanning mode. One challenge here is to mitigate the shadow effects caused by non-uniform illumination penetrating from front layers to back layers. This shadow effect has been observed in several THz-TDS imaging experiments; see e.g., Fig. 3 in [1] and Fig. 9 in [2]. Our own experiment on multi-layer hardboard papers also shows clear evidence of the shadow effect in Fig. 1 (b). Current solutions perform THz multi-layer imaging using a cascade of layer identification and contrast enhancement steps [1], frequency-domain deconvolution [2] or a time-domain sparse deconvolution via the ray-tracing model [3] without explicitly accounting for the shadow effect. In this paper, we propose to mitigate the shadow effect by utilizing recent advances in nonlinear inverse scattering for a complete characterization of the multi-layered sample structure.

II. Problem Formulation and Proposed Scheme

Our approach models the nonlinear relationship between the dielectric permittivity profile and the propagating wavefield according to the scalar theory of diffraction [4]. Consider a scenario where the THz sensor is placed in $(x-y)$ plane of a Cartesian coordinate system and the layered dielectric medium extends in the z-direction. Assume that, as in the raster scanning mode where the wave propagation is one dimensional (1D), a point object placed at a distance r with respect to the transceiver within a bounded depth domain $\Omega \subset \mathbb{R}$ is illuminated by an incident wave $u_{in}(r)$, and that the scattered wave is denoted as $u_{sc}(r), \forall r \in \mathbb{R}$. Using the scalar

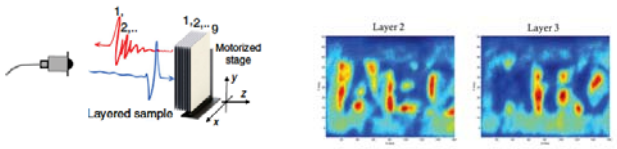

(a) (b)

Fig. 1. THz-TDS multi-layer imaging (from [1]) and (b) the shadow of three letters on the 1st layer is clearly shown on the 2nd layer.

Lippmann-Schwinger equation [4], the relationship between wave and permittivity contrast can be established as

$$u(r) = u_{in}(r) + k^2 \int_{\Omega} g(r-r')u(r')d(r')dr', \forall r \in \Omega, \quad (1)$$

where $u(r)$ is the total field. Note that $d(r) = \epsilon(r) - \epsilon_b$ represents the dielectric permittivity profile, where $\epsilon(r)$ is the permittivity of the object, ϵ_b is the permittivity of the background and k is the THz wavenumber in vacuum. Furthermore, $g(r) = -\frac{i}{2k_b}e^{-ik_b|r|}$ is the 1D free-space Green's function, and $k_b = k\sqrt{\epsilon_b}$ is the wavenumber of the background medium. Note that d is assumed to be real, implying that the object is lossless.

By taking the Fourier transform into frequency domain and discretizing over depth domain z, the measured wavefield in (1) can be reformulated as

$$\begin{aligned} \mathbf{u}(\omega) &= \mathbf{u}_{in}(\omega) + \mathbf{G}(\omega)\mathrm{Diag}(\mathbf{d})\mathbf{u}(\omega), \\ y(\omega) &= \mathbf{h}^T(\omega)\mathrm{Diag}(\mathbf{u}(\omega))\mathbf{d} + e(\omega), \end{aligned} \quad (2)$$

where ω is the angular frequency, $y(\omega)$ is the measurement at ω and $e(\omega)$ is the measurement noise. Furthermore, $\mathbf{h}(\omega)$ represents the 1D Green's function that maps the depth domain Ω to the receiver domain Γ, $\mathbf{G}(\omega)$ is the discretization of Green's function in transmitter to the depth domain, and $\mathbf{d}$ characterizes the depth-domain permittivity profile in Ω.

To recover the depth structure, i.e., the dielectric permittivity, we consider the following nonlinear optimization problem,

$$\begin{aligned} \min_{\mathbf{d},\mathbf{u}} \quad & \sum_{\omega} \mathcal{D}_{\omega}(\mathbf{d},\mathbf{u}) + \mathcal{R}(\mathbf{d}) \\ \text{s.t.} \quad & \mathbf{u}(\omega) = (\mathbf{I} - \mathbf{G}(\omega)\mathrm{Diag}(\mathbf{d}))^{-1}\mathbf{u}_{in}(\omega), \end{aligned} \quad (3)$$

where the data-fidelity term at the frequency ω is given as

$$\mathcal{D}_{\omega}(\mathbf{d},\mathbf{u}) \triangleq \frac{1}{2}\|y(\omega) - \mathbf{h}^T(\omega)\mathrm{Diag}(\mathbf{u}(\omega))\mathbf{d}\|_2^2 \quad (4)$$

and $\mathcal{R}(\mathbf{d})$ is a regularization term over the depth (z) domain and/or spatial $(x-y)$ domains. Particularly, we use

978-1-5386-8285-2/19/$31.00 ©2019 IEEE

a total variation (TV) regularization term $\mathcal{R}(\mathbf{x}) \triangleq \tau\|\mathbf{D}\mathbf{x}\|_1$ to preserve sharp edges in the depth domain, where $\mathbf{D}$ is the discrete finite difference operator in 1D and $\tau > 0$ is a regularization parameter. Note that the above cost function is non-convex due to the constraint in (3). To efficiently tackle the problem, we resort to a quasi-Newton like global optimizer such as limited-memory BFGS (L-BFGS) algorithm [5] and use the alternating direction method of multipliers (ADMM) [6] to handle the regularization term. We first make use of the ADMM algorithm to project our current solution to the TV regularization space and then use it to optimize $\mathbf{d}$ in (3) using L-BFGS without the regularization term.

Furthermore, instead of optimizing (3) over all the frequencies at once, we introduce an incremental frequency inversion optimization framework to refine the estimated permittivity profile [7]. Particularly, with N_ω discrete frequencies, the proposed framework iteratively solves the optimization problem from low frequencies to high frequency (e.g., ω_n) while keeping the individual cost functions at low frequencies (e.g., $\mathcal{D}_i(\mathbf{d}, \mathbf{u}_i), i < n$) as a regularizer for the high frequency as,

$$(\mathbf{d}_n, \mathbf{u}^*) \triangleq \arg\min_{\mathbf{d},\mathbf{u}} \mathcal{D}_\omega(\mathbf{d}, \mathbf{u}_n) + \sum_{i=1}^{n-1} \lambda_i \mathcal{D}_i(\mathbf{d}, \mathbf{u}_i) + \mathcal{R}(\mathbf{d})$$
$$\text{s.t.} \quad \mathbf{u}(\omega) = (\mathbf{I} - \mathbf{G}(\omega)\text{Diag}(\mathbf{d}))^{-1}\mathbf{u}_{in}(\omega), \tag{5}$$

where $n = 1, \cdots, N_\omega$, and $\lambda_i \in (0, 1]$ are regularization parameters that account for the sub-total cost function at lower frequencies ($\omega_i < \omega_n$) into the current cost function at the frequency ω_n. As a result, we sequentially solve N_ω subproblems in (5), and the sequence of solutions iteratively proceed towards the global minimizer of (3) [7].

III. Numerical Simulation Results

The proposed method is numerically evaluated using synthetically generated data with relatively large contrast variation in the object permittivity. In our experiment, we consider a three-layered sample of size 7×7 pixels, each pixel having relative permittivities of 0.3 and 0.8. The thickness of each layer and the air gap between two consecutive layers are 0.3 mm and 0.2 mm, respectively. The sample is placed 5 mm away from the THz transceiver. The transmitted THz waveform covers 240 frequencies up to 1.82 THz. Fig. 2 (a) and (b) show two dielectric constant profiles over the three-layer structure and recovered results, respectively. It is seen that a good recovery of the three-layer structure with small elevated estimates in air gaps in between the layers. The results in Fig. 3 shows mitigated shadow effects of the three-layer imaging. Compared with the existing approach based on layer identification and peak magnitudes (in the middle column of Fig. 3), the results in the right column shows mitigated shadow effects of the three-layer imaging.

IV. Conclusions

The shadow effect in the THz-TDS multi-layer image has been mitigated by using recent advances in nonlinear inverse scattering and by capturing the interaction between the dielectric permittivity profile and the THz wavefield. The proposed method recovers the multi-layer structure by solving a 1D nonlinear inverse scattering model via an iterative and sequential optimization over frequencies. The effectiveness of the proposed method is verified using numerical results.

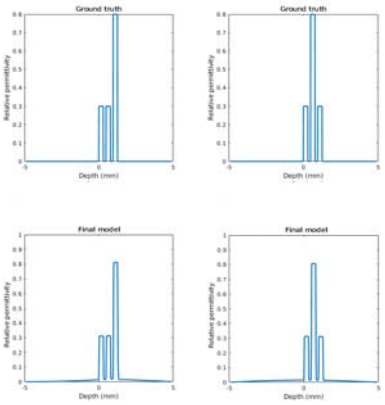

Fig. 2. Synthetic validation on a three-layer sample pixels with dielectric permittivity profiles of (a) [0:3; 0:3; 0:8], (b) [0:3; 0:8; 0:3]

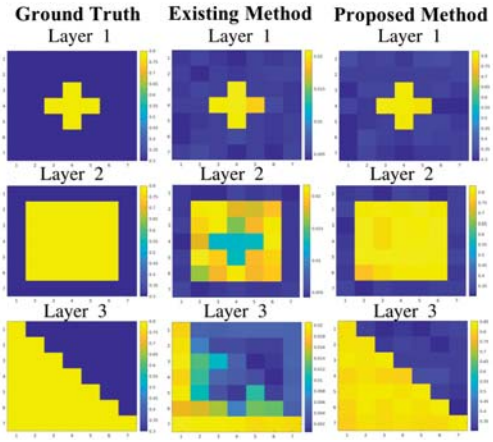

Fig. 3. The sliced view of the layered structure: ground truth, existing method and our shadow removal using our proposed method

References

[1] A. Redo-Sanchez, et al., "Terahertz time-gated spectral imaging for content extraction through layered structures," *Nature Communications*, vol. 7, pp. 1–7, Sept. 2016.

[2] G. C. Walker, et al., "Terahertz deconvolution," *Opt. Express*, vol. 20, no. 25, pp. 27230–27241, Dec 2012.

[3] J. Dong, et al., "Terahertz superresolution stratigraphic characterization of multilayered structures using sparse deconvolution," *IEEE Transactions on Terahertz Science and Technology*, vol. 7, no. 3, pp. 260–267, 2017.

[4] Y. Ma, et al., "Accelerated image reconstruction for nonlinear diffractive imaging," in *Proceedings of the International Conference on Acoustics, Speech, and Signal Processing*, April 2018, pp. 6473–6477.

[5] J. Nocedal, "Updating quasi-newton matrices with limited storage," *Mathematics of Computation*, vol. 35, no. 151, pp. 773–782, 1980.

[6] S. Boyd, et al., "Distributed optimization and statistical learning via the alternating direction method of multipliers," *Found. Trends Mach. Learn.*, vol. 3, no. 1, pp. 1–122, Jan. 2011.

[7] A. Kadu, et al., "Reflection tomographic imaging of highly scattering objects using incremental frequency inversion," in *IEEE ICASSP*, 2019.